ISSN 1063-7761, Journal of Experimental and Theoretical Physics, 2017, Vol. 125, No. 6, pp. 1116–1126. © Pleiades Publishing, Inc., 2017.
Original Russian Text © V.S. Zhandun, V.I. Zinenko, 2017, published in Zhurnal Eksperimental'noi i Teoreticheskoi Fiziki, 2017, Vol. 152, No. 6, pp. 1309–1320.

ORDER, DISORDER, AND PHASE TRANSITION IN CONDENSED SYSTEM

First Principles Investigation of the Magnetic, Magnetoelectric, and Optical Properties of Double Perovskites Containing Ions of Transition Metals $LaPbTSbO_6$ (T = Fe, Co, Ni)

V. S. Zhandun* and V. I. Zinenko

Kirensky Institute of Physics, Siberian Branch, Russian Academy of Sciences,
Akademgorodok 50/38, Krasnoyarsk, 660036 Russia
**e-mail: jvc@iph.krasn.ru*

Received August 23, 2017

Abstract—Within the first principles approach implemented in the VASP package, a correlation between magnetic, electronic, polarization, and optical properties, on the one hand, and the structural ordering of cations, on the other hand, is investigated in double perovskites $LaPbTSbO_6$ (T = Fe, Co, Ni). Two types of cation ordering are considered: simultaneous layered (LL) and checkerboard (RR) ordering of both cations. These two types of ordering are chosen due to their significance; namely, the ordering RR is one of the most implementable types of cation ordering in double perovskites, and compounds with layered ordering can be considered as a heterostructure consisting of periodically alternating metal–nonmagnetic metal layers, which is of interest for experimental synthesis and investigation. It is found that the type of cation ordering in compounds with T = Fe and Ni radically changes the magnetic and/or electronic properties of the compound. Moreover, it is found that low-symmetry stable phases are polar for both types of cation ordering, and the values of spontaneous polarization are evaluated.

DOI: 10.1134/S106377611712010X

1. INTRODUCTION

Modern progress in the growth technology of bulk crystals and thin films has led to growing interest in the search for and development of new advanced materials. One of directions is the search for new materials with appropriate magnetic, optical, and magnetoelectric properties. One of the most advanced materials with suitable properties is perovskite-like compounds, in particular, double perovskites $AABB'O_6$. Compounds with perovskite structure belong to the class of functional materials due to the wide variety of physical properties that they can possess depending on their composition and structure. The investigation of electronic, magnetic, ferroelectric, and magnetoelectric properties of such compounds is of significant experimental and theoretical scientific interest [1–5]. Of great interest are, in particular, double perovskites with magnetic ions in the *A* and/or *B* positions [6–10], since they may exhibit new magnetic and magnetoelectric properties compared with compounds with simple perovskite structure. Various types of cation ordering may lead to a change in the properties of these compounds. The most common type of ordering is the ordering of *B* and *B*' cations in the structure of NaCl (checkerboard ordering of cations). However, simultaneous ordering of cations *A* and *A*' and *B* and *B*' may lead to new functional properties [11]. Moreover, simultaneous ordering of *A* and *B* cations is interesting from the viewpoint of searching for new heterostructures with advanced properties for application in modern electronics. In addition to the applied value, compounds with double perovskite structure are also of interest from the viewpoint of fundamental physics. For example, of interest are the physical mechanisms responsible for one or other physical properties and their relation to the structure and composition. Although most experimentally synthesized double perovskites $AA'BB'O_6$ are either completely disordered, or only cations in the positions *B* are ordered, a first principles calculation allows one to predict the properties of hypothetical ordered compounds that, as a rule, differ from the properties of disordered compounds and, which is no less important, to find out the effect of the type of cation ordering on the physical properties.

Recently, double perovskites $LaPbTSbO_6$ (where T = Mn, Fe, Ni) have been independently synthesized and studied by two experimental groups [1, 2]. Experimentally synthesized compounds have disordered *A* cations and checkerboard ordering of *B* cations. The authors established that all compounds have a nonpolar symmetry group $P2_1/n$ and are antiferromagnetic dielectrics with Néel temperature of about 10 K. In [12], within a first principles approach, we investi-

Table 1. Equilibrium lattice parameters, *a*, and magnetic moments μ of the atoms of transition metals

	$LaPbFeSbO_6$		$LaPbCoSbO_6$		$LaPbNiSbO_6$	
	RR	LL	RR	LL	RR	LL
a, Å	3.99	4.04	4.00	3.98	4.01	3.98
μ, μ_B	3.75	3.68	2.73	2.73	1.78	1.77

gated magnetic and ferroelectric properties of double perovskites $LaPbTSbO_6$ (where T = Mn, Fe, Co, Ni) in a hypothetical ordered structure with the following preferred cation ordering: layered ordering of *A* and *A*' cations and checkerboard ordering of *B* and *B*' cations. We found that such cation ordering gives rise to a low-symmetry polar phase $P2_1$ with simultaneous condensation of the most unstable vibrational modes of the crystal lattice. Thus, we showed that, for a certain cation ordering, these compounds may exhibit spontaneous polarization along with antiferromagnetic ordering of magnetic moments, which suggests the effect of cation ordering on the magnetoelectric properties in double perovskites with this composition.

In the present paper, we present the results of first principles calculations of the structural, magnetic, electronic, and optical properties of ordered double perovskites $LaPbTSbO_6$ (where T = Co, Fe, Ni) in two structural configurations corresponding to different types of simultaneous ordering of cations. This study is intended to find out a relationship between the structural ordering of cations and the magnetic, electronic, optical, and magnetoelectric properties and to predict properties interesting for application in electronics and spintronics.

2. METOD OF CALCULATION

All the calculations were carried out with the use of the VASP package based on the density functional theory for first principles calculations. We used pseudopotentials for plane associated waves, that involve the Perdew–Burke–Ernzerhof (PBE) exchange-correlation functional in the generalized gradient approximation (GGA) [13, 14]. For magnetic ions, we used the following configuration of valence electrons: 3*p*64*s*24*d*6 for a Fe ion, 3*p*64*s*24*d*7 for a Co ion, and 3*p*64*s*24*d*8 for a Ni ion. To calculate the ground state, we used a GGA + U approach in the Dudarev approximation [15], where the value of $U' = U - J$ was chosen equal to 4–6 eV for magnetic ions. All the calculations were performed for spin-polarized states. The integration over the Brillouin zone was performed on a 6 × 6 × 4 Monkhorst–Pack grid [16] with the use of the tetrahedra method with a plane-wave cutoff energy of 500 eV. The lattice parameters and the coordinates of atoms were optimized until the forces at the atoms became less than 0.02 eV.

3. RESULTS AND DISCUSSION

It is known [17, 18] that there are three possible types of ordering of cations in the *A* and *B* positions in double perovskites $AA'BB'O_6$. The most common type of ordering is checkerboard cation ordering (R) along the [111] direction of the perovskite unit cell. In addition, cations can be ordered along the [001] direction, to form the so-called layered cation ordering (L), and along the [110] direction, forming rarely encountered columnar ordering (C).

Simultaneous ordering of the *A* and *B* cations leads to nine possible types of ordered structures [11, 17]. In the present study, we consider two types of ordered structures: simultaneous checkerboard ordering of the *A* and *B* cations (RR) and simultaneous layered ordering of both cations (LR). Note that the second variant of ordering is rarely encountered in nature (examples of compounds with such ordering are given in [17]); however, this type of ordering corresponds to the formation of a heterostructure with alternating layers of magnetic and non magnetic cations, which attracts interest from the viewpoint of tailoring new materials with prescribed properties different from the properties of bulk crystals.

High-symmetry phases of the ordered structures of double perovskites are shown in Fig. 1. For the calculation, we took an eight-times magnified $2a \times 2a \times 2a$ supercell (*a* is the lattice parameter of perovskite) containing 40 atoms. To determine the ground magnetic state, we considered several magnetic configurations: a ferromagnetic (*F*) and three antiferromagnetic (*A*, *C*, *G*) configurations. A schematic view of the antiferromagnetic structures is presented in Fig. 2. For each type of magnetic ordering, we carried out complete optimization of the lattice, which included the optimization of the lattice parameters and atomic coordinates. The optimized lattice parameters are shown in Table 1. The main result of the optimization of atoms in the lattice is the displacement of oxygen ions, which form octahedra around the transition metal and antimony atoms, in the direction of antimony atoms. For example, in the structure with RR cation ordering, the Sb–O distance is 1.98 Å on average, whereas the T–O distance is about 2.1 Å. In the case of the structure with LL ordering, the same distances are 2.05 Å and 2.15 Å, respectively. In addition, the layered ordering of cations exhibits a displacement of the oxygen ions

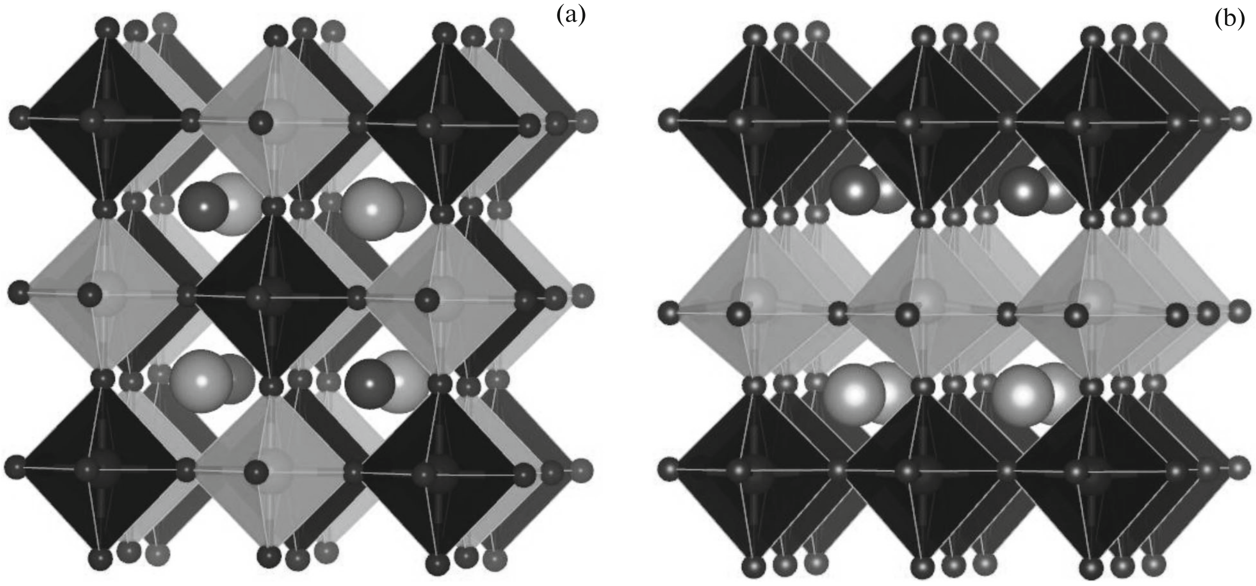

Fig. 1. Structure of the high-symmetry phase; (a) checkerboard cation ordering and (b) layered cation ordering. Dark octahedra represent TO_6, light octahedra, SbO_6, dark balls, Pb, and light balls, La.

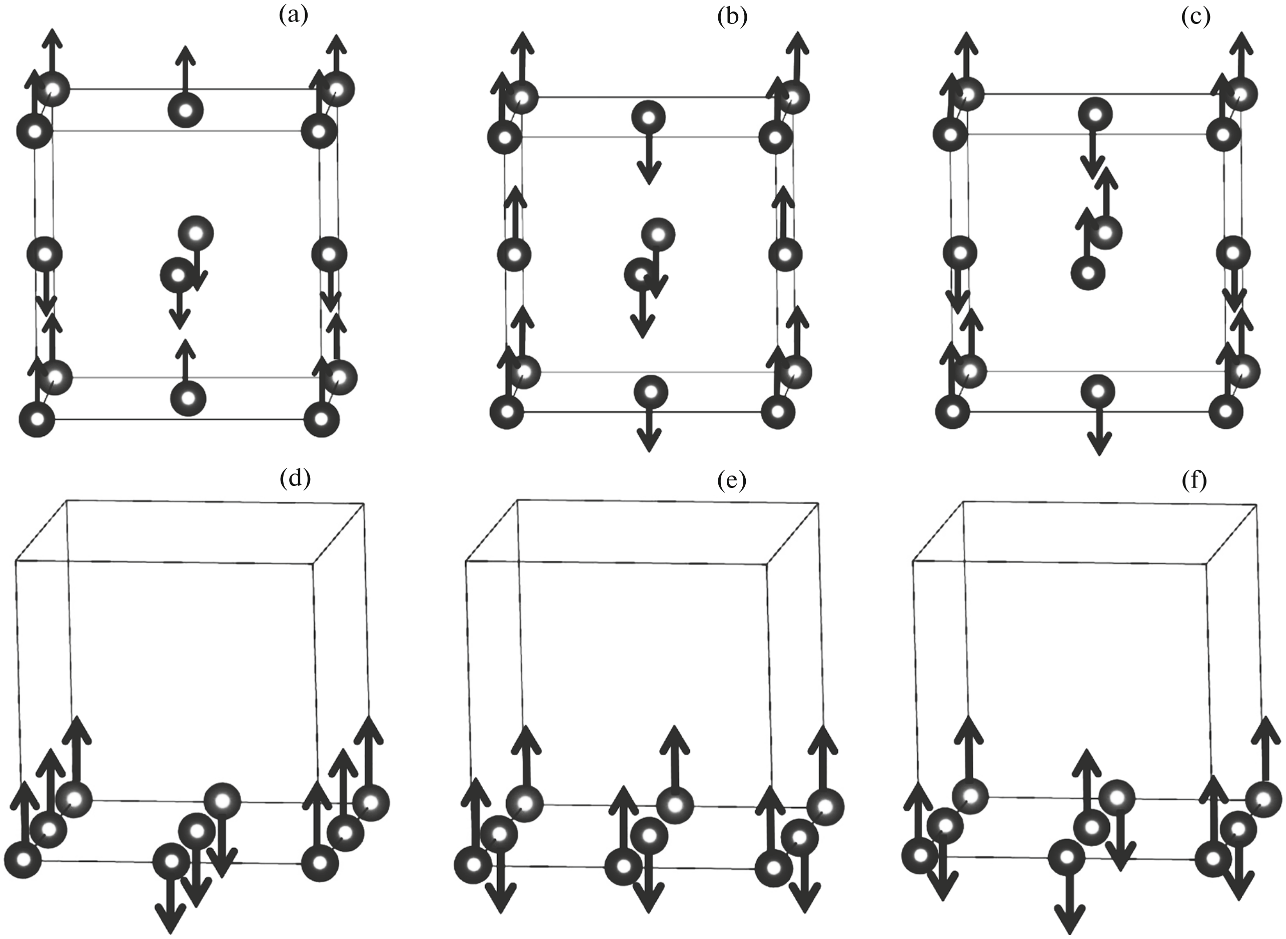

Fig. 2. Schematic view of various magnetic configurations in the case of checkerboard cation ordering; (a) *A* type, (b) *C* type, and (c) *G* type; and in the case of layered cation ordering (d) *A* type, (e) *C* type, and (f) *G* type. Only transition metal atoms are shown.

Table 2. Total energies of various magnetic structures (in eV) for various types of structural ordering of cations

Magnetic structure	$LaPbFeSbO_6$		$LaPbCoSbO_6$		$LaPbNiSbO_6$	
	RR	LL	RR	LL	RR	LL
F	−260.739	−264.657	−253.548	−258.972	−253.315	−253.562
A	−257.000	−264.047	−250.037	−259.142	−244.970	−248.735
C	−257.530	−257.961	−251.202	−258.658	−248.032	−248.564
G	−265.601	−258.164	−258.100	−258.933	−252.645	−249.195

Table 3. Calculated exchange interaction constants between nearest (J_1) and next-to-nearest (J_2) neighbors

	$LaPbFeSbO_6$		$LaPbCoSbO_6$		$LaPbNiSbO_6$	
	RR	LL	RR	RR	LL	RR
J_1, eV	0.027	0.0203	0.065	0.00122	0.012	0.152
J_2, eV	−0.252	0.201	−0.240	−0.0060	0.061	0.0630

forming an oxygen octahedron from the plane of the central atom towards La ions.

The obtained energies and magnetic moments of the structures are given in Tables 1 and 2.

According to Table 2, in $LaPbNiSbO_6$, a ferromagnetic phase is implemented irrespective of cation ordering, while, in $LaPbCoSbO_6$, antiferromagnetic *G* and *A* phases are implemented for the checkerboard and layered cation ordering, respectively. However, in $LaPbFeSbO_6$, the type of magnetic ordering depends on cation ordering: in the case of checkerboard cation ordering, the antiferromagnetic *G* phase is more advantageous, while the layered cation ordering gives rise to a ferromagnetic state. Note that such a relationship between the structure and the magnetic properties was earlier obtained in $LaPbMnSbO_6$ [19].

The electronic properties of the compounds also exhibit dependence on the type of cation ordering. Figure 3 illustrates a comparison of total and partial densities of states for the two types of ordered structures, and Fig. 4 demonstrates a partial density of *d* electrons of transition metals.

In both ordered structures, the main contribution to the occupation of states below the Fermi level is made by the *d* electrons of the transition metal (both *t2g* and *eg*) and *p* electrons of O, which leads to a strong hybridization between the *d* and *p* orbitals of the transition metal and oxygen, respectively. This hybridization near the Fermi level is interesting, in particular, as a factor responsible for the polar distortion of both structures, which will be discussed below. However, while there is an energy gap ranging from 1.8 to 2.3 eV, depending on the magnetic cation *B*, in the density of states of all compounds with checkerboard ordering of both cations, compounds with layered ordering of both cations exhibit metallic properties ($LaPbFeSbO_6$ and $LaPbNiSbO_6$) in addition to dielectric properties ($LaPbCoSbO_6$). The conductivity of $LaPbFeSbO_6$ and $LaPbNiSbO_6$ with layered cation ordering is 0.003 MS/m and 0.001 MS/m, respectively. Moreover, Fig. 4 shows that the energy distribution of *d* electrons depends on cation ordering. For example, a change in the magnetic order due to cation ordering in $LaPbFeSbO_6$ leads to the redistribution of the electron density. In $LaPbNiSbO_6$ and $LaPbCoSbO_6$, where the type of magnetic order is not changed depending on the cation ordering, the main variations are related to the shift in the electron density. This is especially manifest in $LaPbNiSbO_6$, where the density of states of *d* electrons is shifted by the Fermi level, thus giving rise to metallic conductivity.

The exchange interaction constants J_1 and J_2 (between nearest neighbors and next-to-nearest neighbors, respectively) was calculated with the use of the classical Heisenberg Hamiltonian in the form

$$\mathcal{H} = -\frac{1}{2}\sum_{ij} J_{ij} S_i S_j,$$

where J_{ij} is the exchange interaction constant between the *i*th and *j*th sites and S_i and S_j are the effective values of the spin at the *i*th and *j*th sites, respectively. The

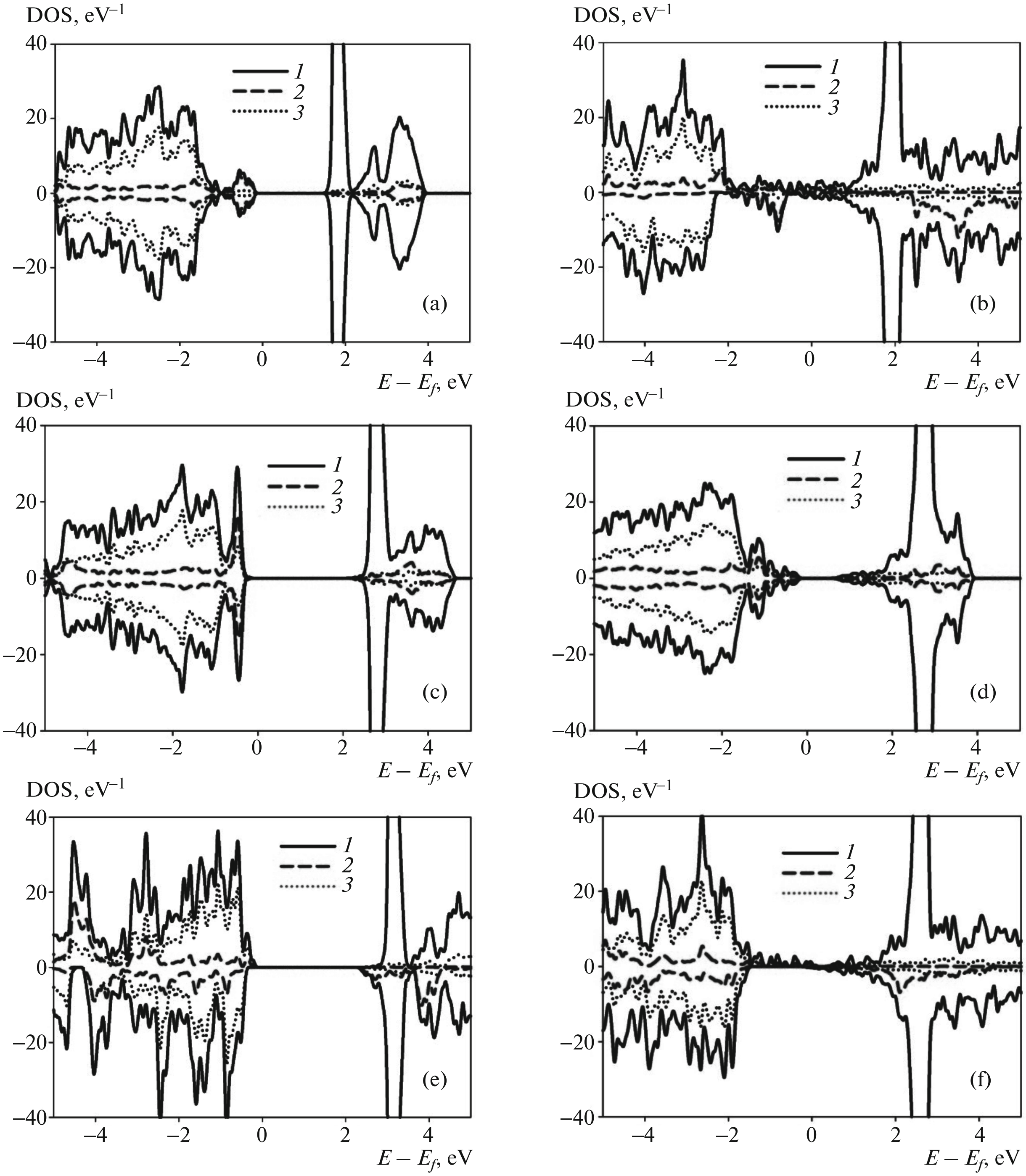

Fig. 3. Partial densities of states of *d* electrons of transition metals; (a) $LaPbFeSbO_6$ in the structure with checkerboard cation ordering, (b) $LaPbFeSbO_6$ in the structure with layered cation ordering, (c) $LaPbCoSbO_6$ in the structure with checkerboard cation ordering, (d) $LaPbCoSbO_6$ in the structure with layered cation ordering, (e) $LaPbNiSbO_6$ in the structure with checkerboard cation ordering, and (f) $LaPbNiSbO_6$ in the structure with layered cation ordering. Curves *1* correspond to the total density of states, curves *2*, to *d* states of transition metal atoms, and curves *3*, to *p* states of oxygen atoms.

equations used to determine the exchange constants for various types of cation ordering are given by

$$E_F = -48J_1 - 24j_2 + E_0,$$

$$E_A = 16J_1 - 24j_2 + E_0,$$

$$E_G = 16J_1 - 8j_2 + E_0$$

for checkerboard cation ordering and

$$E_F = -16J_1 - 16j_2 + E_0,$$

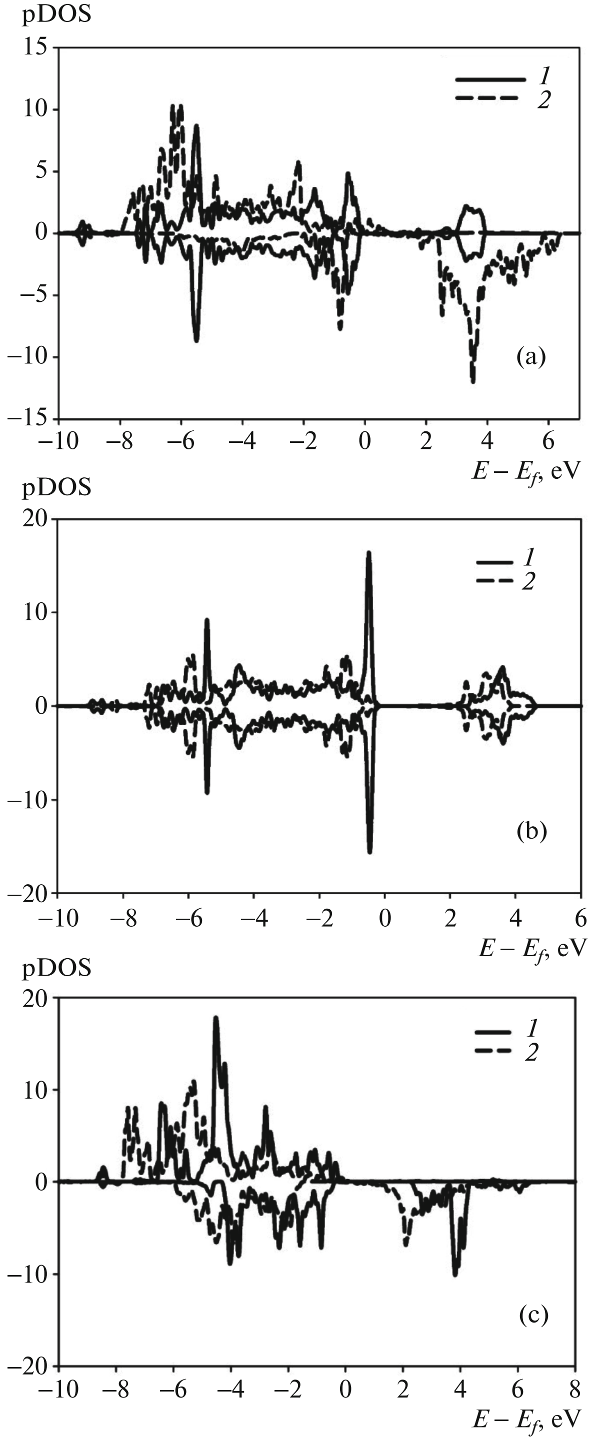

Fig. 4. Partial densities of states of *d* electrons of transition metals (a) $LaPbFeSbO_6$, (b) $LaPbCoSbO_6$, and (c) $LaPbNiSbO_6$ in the structure with checkerboard cation ordering (curves *1*) and in the structure with layered cation ordering (curves *2*).

$$E_A = 16j_2 + E_0,$$

$$E_G = 16J_1 - 16j_2 + E_0$$

for layered cation ordering. Here E_0 is the energy of the paramagnetic phase, and F, A, and G are the energies of magnetic configurations from Table 2. The calculated values of exchange interaction parameters are given in Table 3.

The table shows that, in all cases, the constant J_1 promotes ferromagnetic ordering of magnetic moments; however, in the compounds with antiferromagnetic ordering, the key constant is J_2, which promotes an antiferromagnetic configuration of magnetic moments; moreover, the value of this constant is several times greater than the ferromagnetic constant J_1.

To analyze the instability of the lattice of the high-symmetry phase, we calculated the phonon vibration frequencies, which exhibited a strong instability of the system with respect to lattice distortions: there are a few unstable vibrational modes in the spectrum of the crystal lattice (the frequencies of “soft” vibrational modes at the center of the Brillouin zone are shown in Table 4).

A detailed symmetry analysis of unstable vibrational modes for double perovskites with different types of cation ordering and an analysis of low-symmetry structures were carried out in [11]. Therefore, we present only the final result in the present paper. To determine low-symmetry structures corresponding to the ground state, we distorted high-symmetry phases with respect to the combination of eigenvectors of the most unstable vibrational modes and performed a complete optimization of the structures. As a result, we obtained stable low-symmetry structures possessing the polar symmetry groups $R3$ and Pa for cation ordering RR and LL, respectively.

The structural distortion in the low-symmetry phase is small compared with that in the high-symmetry phase; further calculations showed only slight differences in the behavior of electronic, magnetic, and optical properties of the high- and low-symmetry phases; namely, the dependence of the magnetic and electronic properties of the compounds on the composition and cation ordering is preserved.

In the polar phase, we calculated the value of spontaneous polarization by the formula

$$P_\alpha = \frac{1}{V}\sum Z_{\alpha\beta}u_\beta,$$

where $Z_{\alpha\beta}$ are dynamic Born charges and u_β is the displacement of ions in the low-symmetry phase with respect to the ions in the high-symmetry phase. The results obtained for dielectric compounds are shown in Table 5.

Thus, the presence of spontaneous polarization along with the magnetic order in double perovskites $LaPbTSbO_6$ (T = Fe, Co, Ni) suggests that one can expect a magnetoelectric effect in these compounds. The presence of polar distortions in a compound with

Table 4. Frequencies of unstable modes at the center of the Brillouin zone (cm^{-1})

$LaPbFeSbO_6$		$LaPbCoSbO_6$		$LaPbNiSbO_6$	
RR	LL	RR	LL	RR	LL
220i (A_{1u})	218i (A_{1u})	235i (A_{1u})	246i (E_g)	219i (E_g)	201i (A_{1u})
219i (E_g)	143i (E_g)	219i (E_g)	141i (A_{1u})	187i (E_u)	132i (E_g)
147i (A_{1u})	111i (A_{1u})	158i (E_u)	119i (A_{1u})	139i (A_{1u})	112i (A_{1u})
136i (E_u)	75i (E_u)	123i (A_{1u})	65i (E_u)	125i (E_g)	82i (E_u)
132i (E_g)	57i (E_g)	114i (E_g)	52i (E_g)	98i (A_{1u})	47i (E_g)

metallic properties may seem strange; however, the authors of [20–22] have recently demonstrated the presence of ferroelectric distortions in the metallic compound $LiOsO_3$.

In the concluding part of the study, we present the calculated optical properties of double perovskites $LaPbTSbO_6$ in two ordered structures. The optical properties of a substance can be described by the dispersion of the dielectric function ε(ω). The knowledge of the real (ε') and imaginary (ε'') parts of the dielectric function allows one to calculate various optical characteristics, such as the refractive index (n), the extinction coefficient (k), the loss function (L), the absorption coefficient (α), and the reflection coefficient (R). The real and imaginary parts of the dielectric function were obtained within first principles calculations, while other optical characteristics were calculated by the expressions (1)–(5):

$$n = \sqrt{\frac{|\varepsilon| + \varepsilon'}{2}}, \quad (1)$$

$$k = \sqrt{\frac{|\varepsilon| - \varepsilon'}{2}}, \quad (2)$$

$$R = \frac{(n-1)^2 + k^2}{(n+1)^2 + k^2}, \quad (3)$$

$$L = \frac{\varepsilon''}{|\varepsilon|}, \quad (4)$$

$$\alpha = \frac{2wk}{c}. \quad (5)$$

Table 5. Spontaneous polarization in the low-symmetry phase (P)

	$LaPbFeSbO_6$	$LaPbCoSbO_6$		$LaPbNiSbO_6$
	RR	LL	RR	RR
P, μC/cm^2	23	33	27	31

The results obtained are shown in Figs. 5–7.

Note that, irrespective of the cation ordering, the optical spectra differ little qualitatively: the number and the position of peaks remains the same. Differences are observed only in the intensity and the smearing of peaks. For example, in $LaPbFeSbO_6$, which is dielectric in the case of checkerboard ordering and metal in the case of layered ordering, the peaks for layered ordering turn out to be more smeared and have lower intensity. A characteristic feature of the optical spectra is the presence of a large peak in the imaginary part of the dielectric function for energy of about 5 eV for all compounds with different types of cation ordering; this is associated with a qualitatively similar energy dependence of the electronic density of states for all compounds.

4. CONCLUSIONS

Within the density functional theory implemented in the VASP package, we have carried out first principles calculations of the polarization, magnetic, electronic, and optical properties of hypothetical ordered double perovskites $LaPbTSbO_6$ (T = Fe, Co, Ni). We have considered two ordered structural configurations with simultaneous ordering of A and B cations: layered ordering and checkerboard ordering. The first type of ordering attracts interest due to the presence of alternating nonmagnetic metal–magnetic metal layers, which can be implemented in the form of a heterostructure. The calculation has shown that there is a relationship between the structure and composition of double perovskites $LaPbTSbO_6$, on the one hand, and their polarization, magnetic, electronic, and optical properties, on the other. For example, while $LaPbCoSbO_6$ with checkerboard and layered ordering of both A and B cations is an antiferromagnetic dielectric, $LaPbFeSbO_6$ and $LaPbNiSbO_6$ exhibit ferromagnetic and metallic properties for layered ordering and, for checkerboard ordering, the first is an antiferromagnetic dielectric, and the other is a ferromagnetic dielectric. Thus, the variation of the composition and structure allows one to tailor a

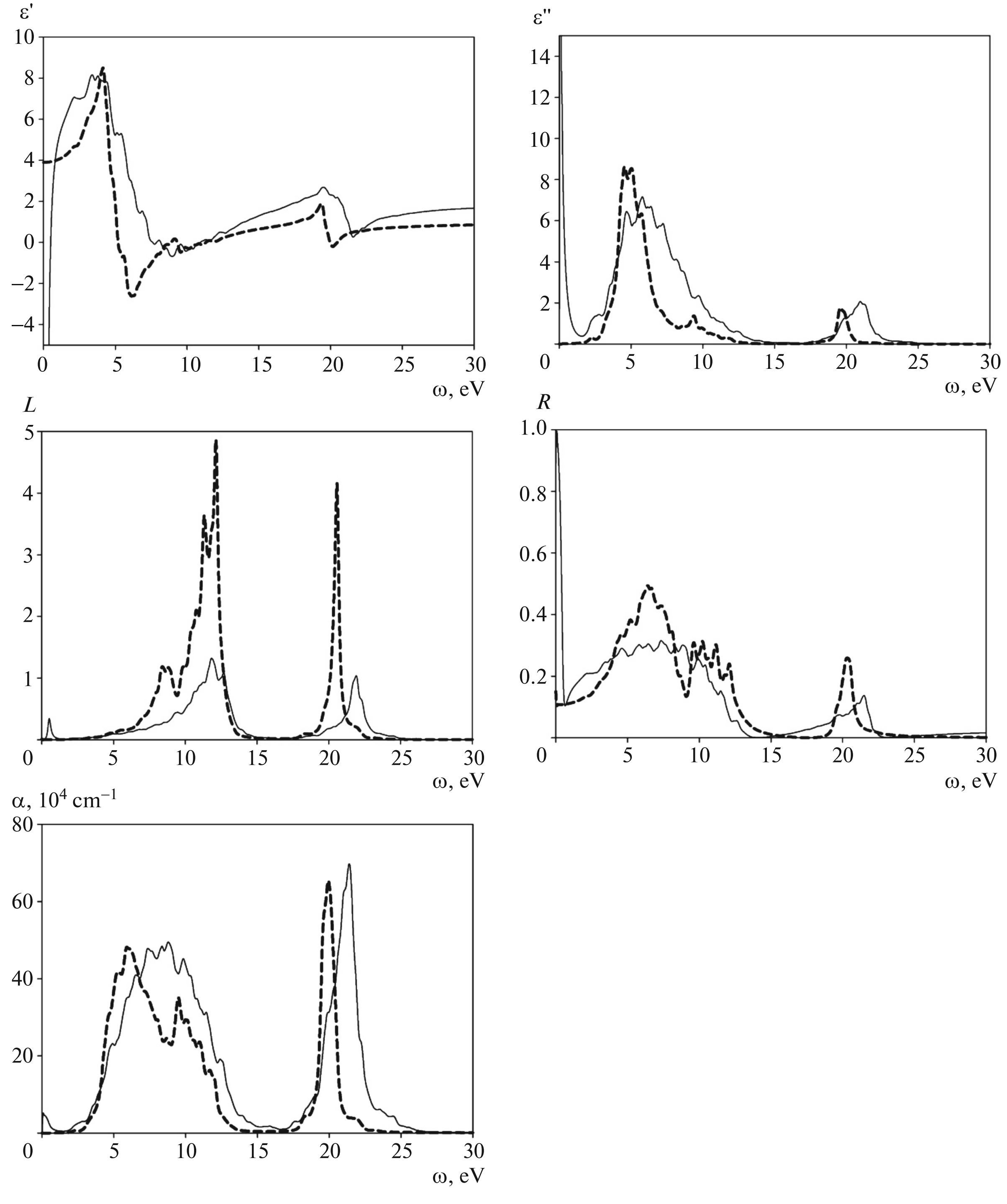

Fig. 5. Optical characteristics of the double perovskite $LaPbFeSbO_6$ in two ordered structures; layered cation ordering (solid line) and checkerboard cation ordering (dashed line).

material with the properties required for applications in electronics and spintronics. We have also found the existence of a low-symmetry polar phase in all the compounds considered, which is associated with the condensation of the most unstable vibrational modes, and evaluated the value of spontaneous polarization in the polar phase, which is on the order of 20 $\mu C/m^2$.

We assume that the results obtained will be of interest both from fundamental and applied (for example, in spintronics) viewpoints.

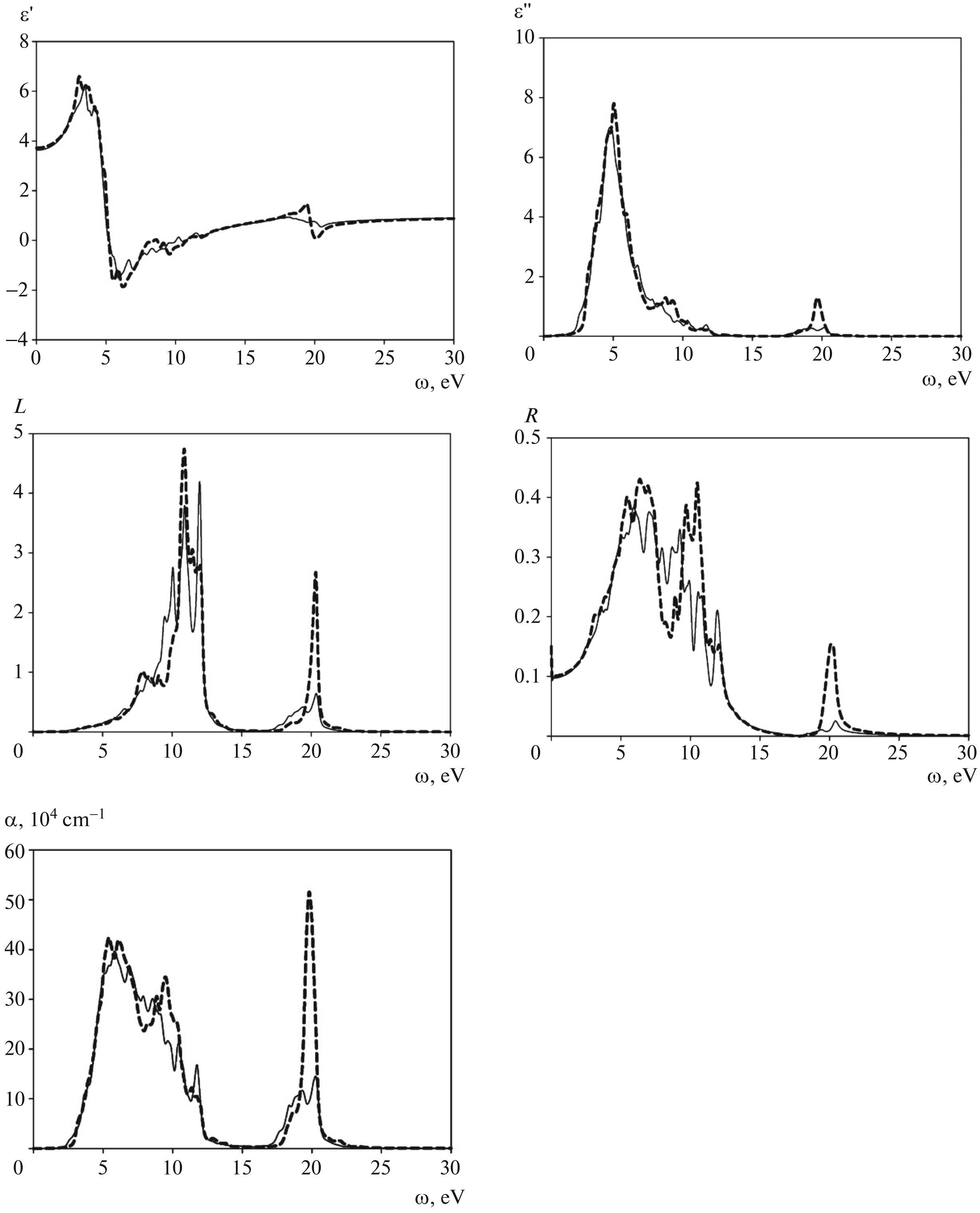

Fig. 6. Optical characteristics of the double perovskite $LaPbCoSbO_6$ in two ordered structures; layered cation ordering (solid line) and checkerboard cation ordering (dashed line).

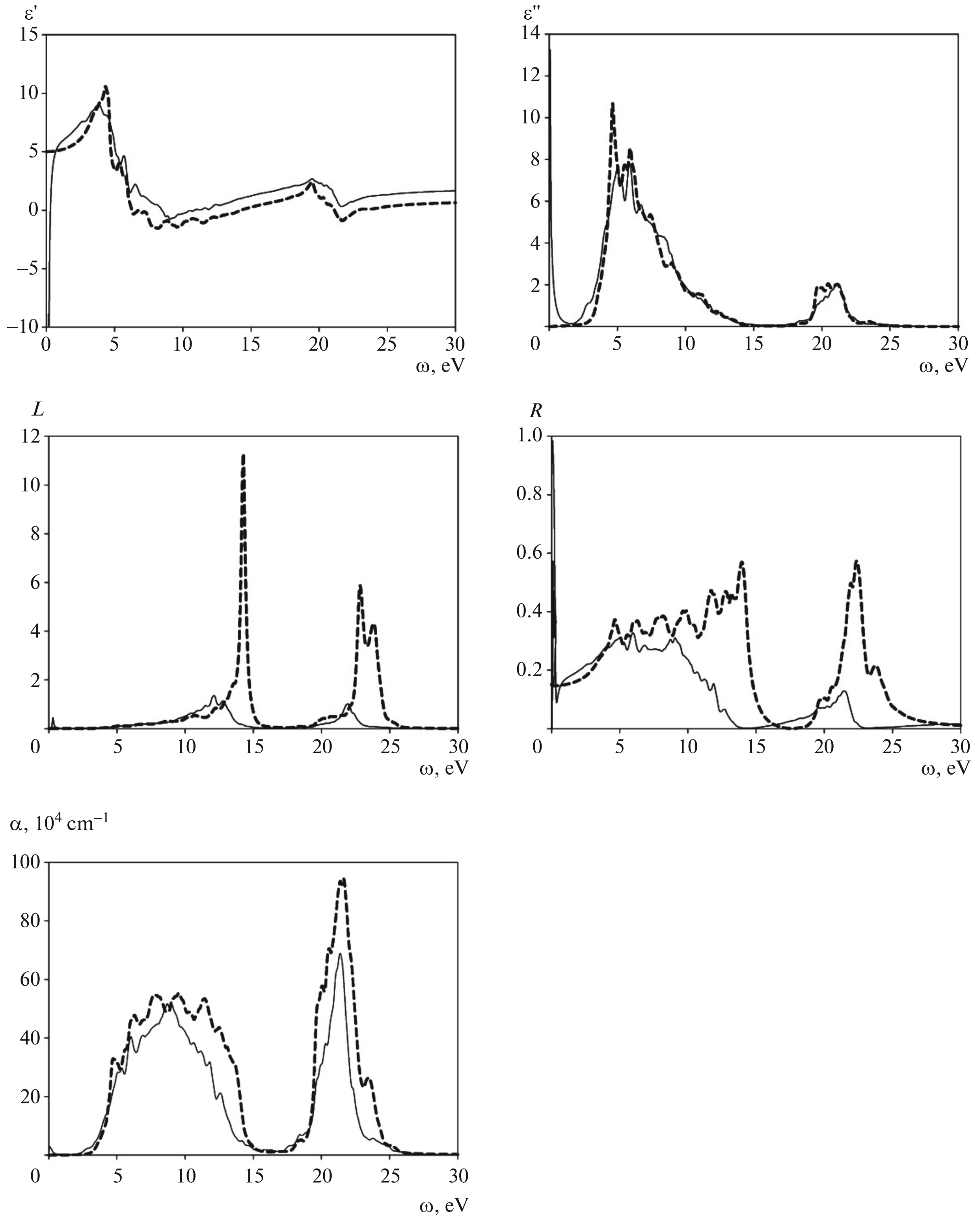

Fig. 7. Optical characteristics of the double perovskite $LaPbNiSbO_6$ in two ordered structures; layered cation ordering (solid line) and checkerboard cation ordering (dashed line).

ACKNOWLEDGMENTS

This work was supported by the Russian Foundation for Basic Research, project no. 15-02-00340, and by the Government of Krasnoyarsk Krai and Krasnoyarsk Krai Fund for the Support of Research and Development (project no. 16-42-243035). The calculations were carried out on the computing facilities of the National Research Center Kurchatov Institute (ui2.computing.kiae.ru).

REFERENCES

1. Y. Bai, L. Han, X. Liu, X. Deng, X. Wu, C. Yao, Q. Liang, J. Meng, and J. Meng, J. Solid St. Chem. **217**, 64 (2014).
2. D. G. Franco, R. E. Carbonio, and G. Nieva, IEEE Trans. Magn. **49**, 4594 (2013).
3. G. Vaitheeswaran, V. Kanchana, and A. Delin, Appl. Phys. Lett. **86**, 032513 (2005).
4. D. Stoeffler and C. Etz, J. Phys.: Condens. Matter **18**, 11291 (2006).
5. S. Gong, P. Chen, and B. G. Liu, J. Magn. Magn. Mater. **349**, 74 (2014).
6. D. A. Landínez Téllez, D. P. Llamosa, C. E. Deluque-Toro, A. V. Gil Rebaza, and J. Roa-Rojas, J. Mol. Struct. **1034**, 233 (2013).
7. D. Serrate, J. M. De Teresa, and M. R. Ibarra, J. Phys.: Condens. Matter **19**, 023201 (2007).
8. Y. Fujioka, J. Frantti, and M. Kakihana, J. Phys. Chem. B **110**, 777 (2006).
9. Y. Zhang and V. Ji, J. Phys. Chem. Solids **73**, 1116 (2012).
10. Q. Zhang, G. H. Rao, Y. G. Xiao, H. Z. Dong, G. Y. Liu, Y. Zhang, and J. K. Liang, Physica B **381**, 233 (2006).
11. N. G. Zamkova, V. S. Zhandun, and V. I. Zinenko, Phys. Status Solidi B **250**, 1888 (2013).
12. V. S. Zhandun and V. I. Zinenko, Phys. Solid St. **57**, 987 (2015).
13. G. Kresse and J. Furthmüller, Phys. Rev. B **54**, 11169 (1996).
14. J. P. Perdew, K. Burke, and M. Ernzerhof, Phys. Rev. Lett. **77**, 3865 (1996).
15. S. L. Dudarev, G. A. Botton, S. Y. Savrasov, C. J. Humphreys, and A. P. Sutton, Phys. Rev. B **57**, 1505 (1998).
16. H. J. Monkhorst and J. D. Pack, Phys. Rev. B **13**, 5188 (1976).
17. G. King and P. M. Woodward, J. Mater. Chem. **20**, 5785 (2010).
18. T. Fukushima, A. Stroppa, S. Picozza, and J. M. Perez-Mato, Phys. Chem. Chem. Phys. **13**, 12186 (2011).
19. V. S. Zhandun and V. I. Zinenko, J. Alloys Compd. **671**, 184 (2016).
20. H. J. Xiang, Phys. Rev. B **90**, 094108 (2014).
21. Youguo Shi, Yanfeng Guo, Xia Wang, A. J. Princep, D. Khalyavin, et al., Nat. Mater. **12**, 1024 (2013).
22. G. Giovannetti and M. Capone, Phys. Rev. B **90**, 195113 (2014).

Translated by I. Nikitin